AR-010-134

DSTO-TR-0492

Elastic-Plastic Analysis of a Plate of Strain Hardening Material with a Central Circular Hole – Comparison of Experiment with Finite Element Analysis Containing the Unified Constitutive Material Model

Robert B. Allan

DEPARTMENT OF DEFENCE

DEFENCE SCIENCE AND TECHNOLOGY ORGANISATION

Elastic-Plastic Analysis of a Plate of Strain Hardening Material with a Central Circular Hole - Comparison of Experiment with Finite Element Analysis Containing the Unified Constitutive Material Model

Robert B. Allan

Airframes and Engines Division
Aeronautical and Maritime Research Laboratory

DSTO-TR-0492

ABSTRACT

This report presents an experimental validation of elastic-plastic finite element stress analysis, using a unified constitutive model to describe the plastic response. The validation was done by experimentally measuring the elastic-plastic strain distribution around a circular hole in a flat plate under tensile loading and comparing it with that produced by a finite element analysis of the specimen using the unified constitutive model. The validation involved strain measurements using both strain gauges and full-field photoelasticity. The unified constitutive model was found to provide a significant improvement over classical plasticity modelling for the case of monotonic loading. A similar validation for cyclic plasticity has not yet been undertaken.

RELEASE LIMITATION

Approved for public release

DEPARTMENT OF DEFENCE

DEFENCE SCIENCE AND TECHNOLOGY ORGANISATION

Published by

DSTO Aeronautical and Maritime Research Laboratory
PO Box 4331
Melbourne Victoria 3001

Telephone: (03) 9626 7000
Fax: (03) 9626 7999

AR-010-134.
February 1997

APPROVED FOR PUBLIC RELEASE

Elastic-Plastic Analysis of a Plate of Strain Hardening Material with a Central Circular Hole - Comparison of Experiment with Finite Element Analysis Containing the Unified Constitutive Material Model

Executive Summary

Accurate estimation of the fatigue lives and/or inspection intervals (based on crack growth rates) in the RAAF's fleets of ageing aircraft is vital for the maintenance of their structural integrity. For some structural features a knowledge of elastic-plastic stress distributions under normal service loads and residual stresses resulting from extreme load cycles is required for an accurate prediction of airframe life.

An area of major concern in the F-111 is the wing pivot fitting manufactured from D6ac steel, which under cold proof load test, experiences extensive plastic deformation and resulting residual stresses. There have been numerous incidents of fatigue cracks at fuel flow vent hole #13 (FFVH13) in the wing pivot fitting in the RAAF F-111 fleet, and the problem could compromise the structural integrity of the fleet up to the planned withdrawal date of 2020 unless properly characterised and managed.

AMRL will provide a refined stress analysis of FFVH13 as part of the RAAF's durability and damage tolerance analysis (DADTA) of the F-111 airframe.

This report is a validation of the elastic-plastic stress analysis methodology using a unified constitutive material behaviour model to determine the stress history and the residual stress at FFVH13 resulting from cold proof load testing of the F-111 airframe.

The report compares the experimental and finite element results (using both a unified constitutive model and a classical plasticity model) for a simple rectangular plate specimen with a central circular hole. The results showed a distinct improvement in prediction using the unified constitutive model over classical plasticity. Typically this improvement was of the order of 10% but in some cases higher. Of more importance is the very good correlation of the unified constitutive finite element results with the experiment, which typically was higher than 94%.

Further work is required to validate the unified constitutive model for cyclic plasticity. This will be the subject of a separate report.

Authors

Robert B. Allan
Airframes and Engines Division

Robert Allan completed a B.E. (Aeronautical) at R.M.I.T. in 1978. Since then he has worked in the areas of aircraft structural design, repair and manufacturing at major Australian and U.S. aircraft companies. Some major projects worked on in this time were the tailplane and elevator design of the Wamira aircraft project, F-18 aft fuselage redesign and the support of local manufacture of numerous aircraft components. Prior to joining AMRL in 1994, he spent 5 years in the field of polymer flow characterisation and simulation using finite element methods gaining a broad knowledge of finite element stress analysis. Since joining AMRL he has worked in the area of life extension through the use of structural mechanics in support of Australian Defence Force aircraft, specialising in finite element stress analysis and advanced experimental stress analysis.

Contents

1. Introduction

AMRL has been tasked by the RAAF to investigate methods of improving the fatigue life of the F-111 airframe. Figure 1 shows an area on the F-111 aircraft under investigation at AMRL. It is in the wing pivot fitting that is made from D6ac steel. This area is known as fuel flow vent hole number 13 (FFVH13) and is located in stiffener number 3 inside the upper wing plate of the wing pivot fitting. A vertical titanium shear web is attached to this stiffener. This area is highly loaded due to the bending and shear at the wing root and the hole causes additional high stress concentration. There have been numerous incidences of cracks developing at the lower inboard corner of FFVH13 in the Royal Australian Airforce's (R.A.A.F.'s) F-111 fleet.

As part of its structural integrity program, the F-111 aircraft is subjected to periodic cold proof load tests (CPLTs), in which positive and negative limit load cycles are applied to the wings at -40°F (-40°C) and at two wing sweep angles. The CPLTs cause localised plastic deformation at many locations in the wing pivot fitting, including FFVH13. The resulting high residual tensile stresses at FFVH13 cause fatigue cracks to develop at a location which is otherwise compression dominated for positive flight load cycles. In order to determine safe inspection intervals for this location the R.A.A.F. tasked AMRL to accurately determine the residual stresses after CPLT and the cyclic stresses from service loading.

Determining residual stresses after CPLT is a challenging task because it involves two complete load cycles to high magnitude positive and negative plastic strains. AMRL approached this task by developing a unified constitutive material behaviour model for D6ac steel (Reference 1), implementing that model in a finite element code PAFEC (Reference 2) and using it to analyse a sub-structure model of FFVH13 (Reference 3). This report describes an investigation to validate the D6ac steel constitutive model and its implementation into PAFEC.

A plate specimen with a round hole was employed to validate the constitutive model in a biaxial stress field. This report describes monotonic static tests on the plate specimen with a round hole to determine its strain versus load response and compares it to that predicted from a finite element analysis of the specimen. Analytical solutions (References 4 and 5) are also available for this problem to compare with the experimental and finite element results.

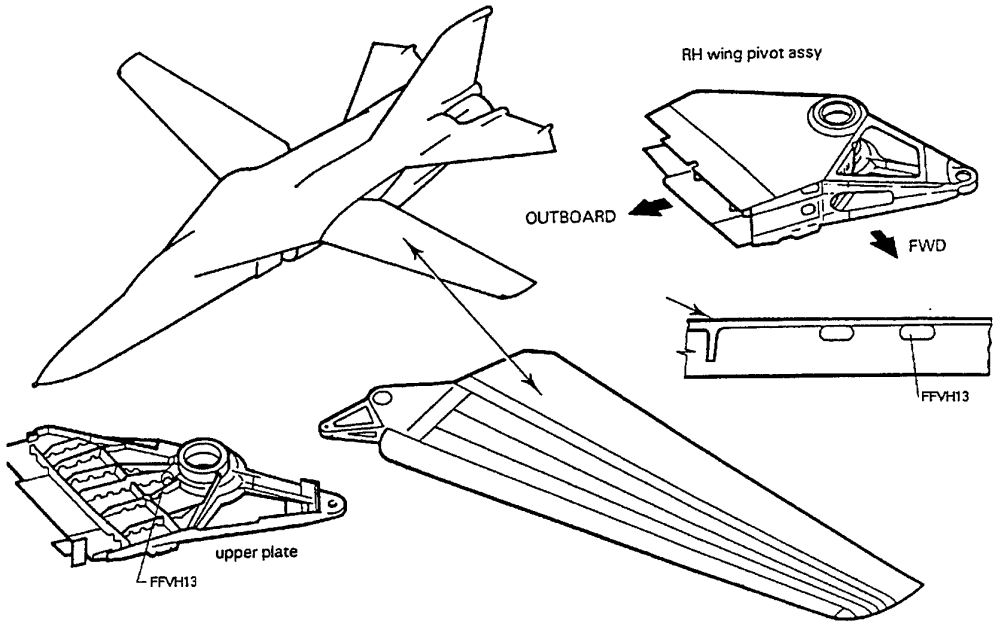

Figure 1: F111 Aircraft & wing, showing location of critical hole, FFVH13

Strain gauge results from a full scale wing test (Reference 6) at FFVH13 gave a maximum strain of 7888 με in tension (-3 g down load), and a maximum strain of -21459 με in compression (+7.3 g up load).

2. Test Specimen

A round hole test specimen was made from existing D6ac steel plates. Figure 2 gives the dimensions of the specimen.

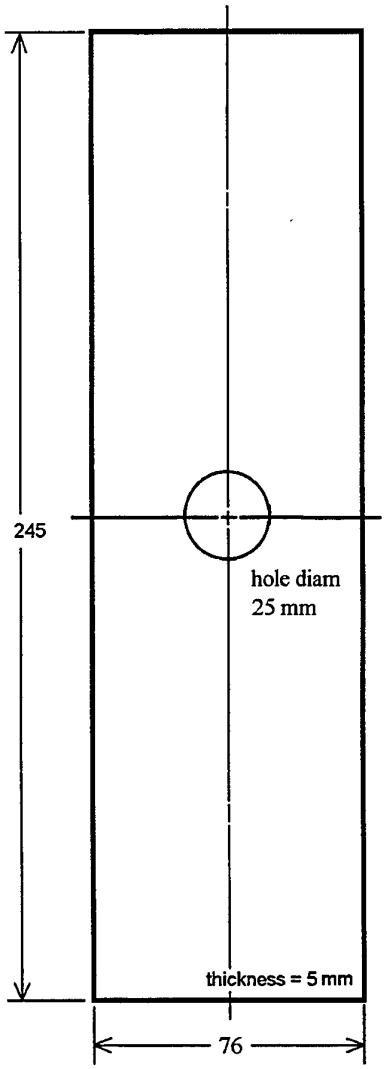

Figure 2: Geometry of test specimen

Strain gauges were fitted to the specimen as shown in Figures 3 and 4. Table 1 gives the locations of the gauges. Figure 3 has the predicted yield zone growth superimposed on it. The preliminary finite element analysis carried out to predict this yield growth is not presented in this report as it was only used to gain an insight into locating the strain gauges in the higher strain regions. No work is done in this report to predict the elastic-plastic boundary or to measure it.

Table 1 : Distance of strain gauges from reference point A, Figure 3.

Gauge number	1	2	3	4	5	6	9	10	11	12
distance [mm] from point A	1.5	4.5	8	5	11.5	17.5	12	15.5	24	30

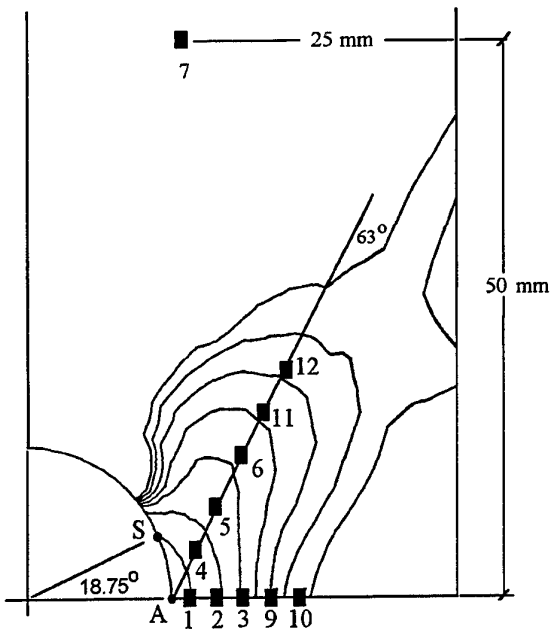

Figure 3: Location of strain gauges in relation to predicted yield zone growth. Gauge 8 is opposite the vertical centre line to gauge 7. The strip gauge is centred on point S and extends nominally 41° to either side (refer Figure 4).

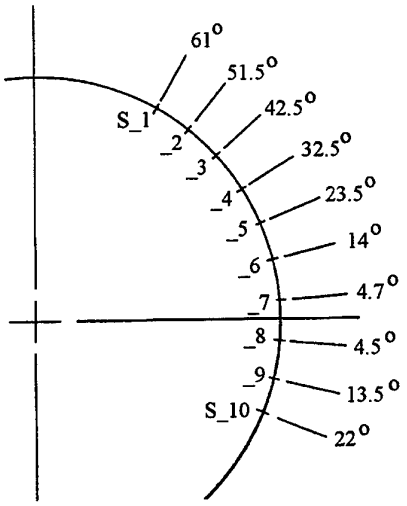

Figure 4: Location of strip gauge elements around inside of hole.

Photoelastic coatings were applied as shown in Figure 5 to provide a visual, full-field method of measuring the plastic zone growth. They were also to be used as a back-up to the strain gauge data. They were applied to the opposite face of the specimen from

the strain gauges. Various thicknesses were used. Each thickness covered a quadrant of the specimen and they were therefore measuring the same stress distribution. Each thickness has a different sensitivity to strain so a wide range of strains could be measured during loading.

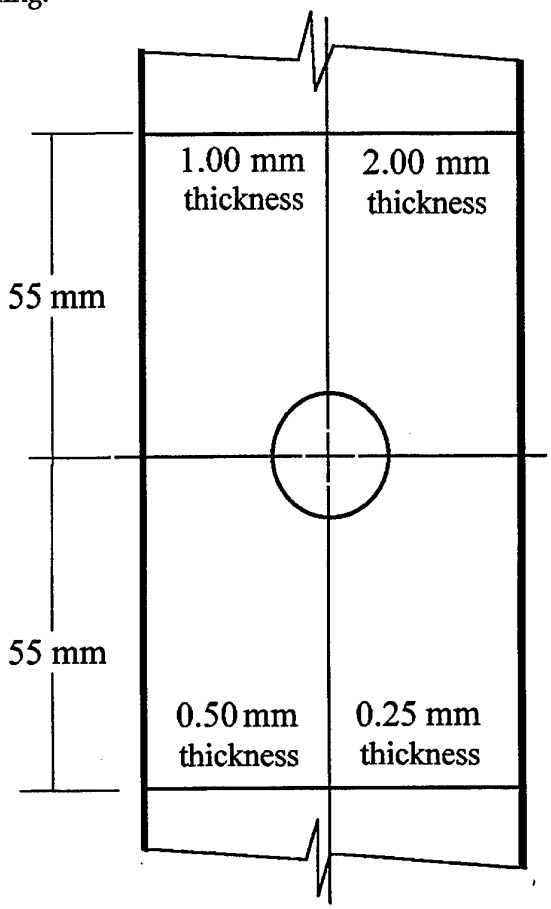

Figure 5: Location and thicknesses of photoelastic coatings.

A clip gauge (extensometer) was installed via two thick aluminium blocks adhered to the specimen on the same face as the strain gauges (Figure 6). These blocks were larger than ideal, as will be demonstrated later (Section 7), and tended to average the strains over the adhered block length.

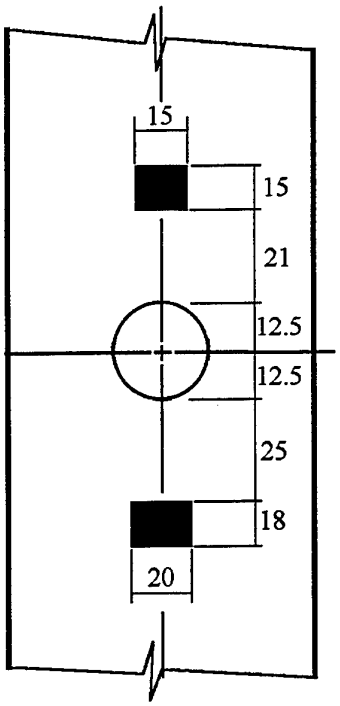

Figure 6: Location of blocks adhered to specimen for connection of clip gauge. Knife edges were placed mid-way along blocks - gauge length was 87.5mm

3. Loading

The load required to achieve the -21459 με strain in compression would have caused the specimen to buckle. The maximum strain before buckling was estimated as -10,576 με. It was decided not to use this low compressive strain, that was only about 4000 με above the yield, as only a small plastic zone would have been created. Instead, the specimen was loaded monotonically in tension to sufficient load to create large areas of plasticity.

Tensile loading (in kN) was to be done in steps up to +375 kN as follows:

0, 37.5, 75, 113, 150, 187, 225, 264, 300, 338, 375 , 338, 300, 262, 225, 188, 150, 113, 75, 37, 0

The loading rate was set at 0.5 kN/sec - this equates to approximately 6.3 με/sec in the specimen remote from the hole. Figure 7 shows the strain rate present at the hole edge due to this applied load rate - around 22 με/sec over the linear part of the curve, indicating a strain concentration factor of 3.5 .

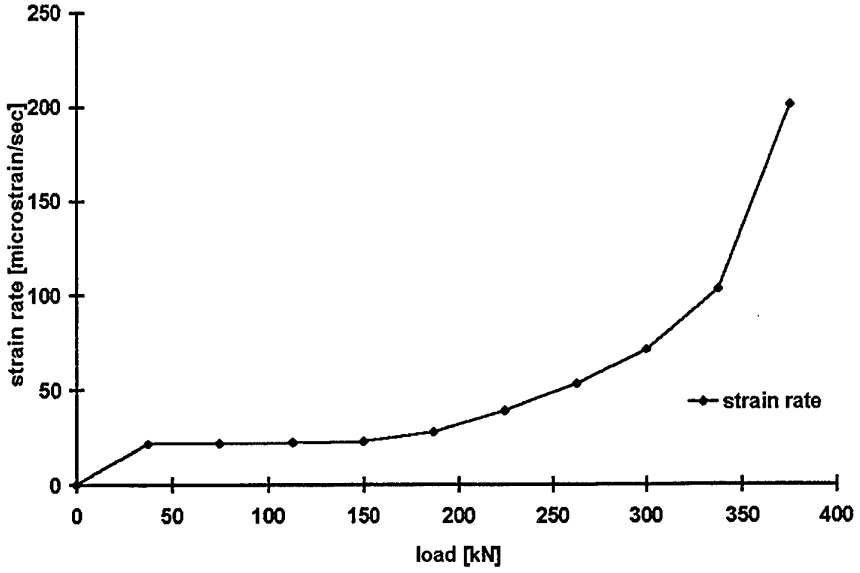

Figure 7: Experimental strain rate at the hole edge, gauge element S_8.

4. Test Method

The specimen was placed in the top jaws of the testing machine and aligned. A clip gauge was attached to the aluminium blocks on the specimen to measure overall specimen deflection. Strain readings and photographs of the photoelastic fringe patterns were taken every 37 kN (approx.) - this is equivalent to every 100 MPa (approx.) in terms of nominal stress.
Loading continued in tension until gauges numbers 1 & 4 began to indicate what was thought to be high local yielding instability. It was in fact gauge failure at high strains.

5. Finite Element Analysis

An elastic-plastic plane stress finite element analysis of the specimen was performed using PAFEC level 8.1 with the unified constitutive material model as reported in Reference 1. This is development code and no release number is available. Eight noded isoparametric elements (PAFEC type 36210) were used. The finite element analysis was run with the standard classical plasticity available in PAFEC as well as the new unified constitutive plasticity as a comparison. The run dates of the analyses were May 1 & 3, 1996. The code was run on AMRL's Hewlett Packard K series 9000 computer.

Because of symmetry, a quarter of the specimen was modelled with suitable boundary conditions to simulate a full plate as shown in Figure 8. A thickness of 5mm was used. Unloading was not simulated. Refer to Appendices A and B for PAFEC data files used for the classical and unified constitutive analyses respectively.

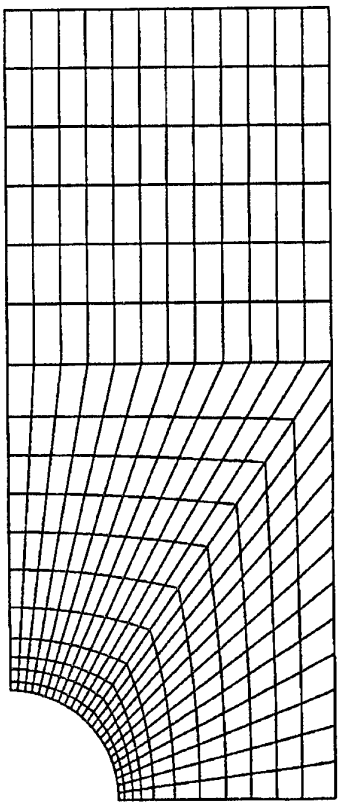

Figure 8: Quarter Finite Element model used in analysis.

6. Test Results

The raw data from the test are included in Tables 2 to 5. Note: zero load strains are due to specimen clamp-up; gauges were zeroed prior to clamp-up.

Table 2: Experimental results for round hole specimen

Load	Clip	Clip	Gauge Number				
	Gauge	Displ't	1	2	3	4	5
kN	με	mm	με	με	με	με	με
0.0	-30481	0.04	-350	-308	-360	-53	-162
37.5	-31152	0.20	878	528	325	345	539
75.1	-31851	0.37	2108	1361	1003	744	1247
112.9	-32559	0.55	3367	2221	1702	1150	1971
150.0	-33262	0.74	4598	3054	2383	1550	2682
187.0	-33978	0.94	5941	3913	3074	1969	3409
224.8	-34726	1.16	7878	4916	3818	2448	4170
262.8	-35516	1.40	10648	6350	4686	3051	4970
299.9	-36359	1.66	14440	8690	5855	3920	5733
337.7	-37397	2.88	20170	12507	8013	5235	6539
374.9	-39339	4.69	18112	21700	13146	5455	8721
374.9	-39408	4.70	15427	22087	13353	5034	8811
375.0	-39457	4.70	14620	22367	13501	4644	8884
374.9	-39494	4.71	14256	22564	13607	4433	8939
375.0	-39524	4.72	14016	22719	13690	4312	8980
337.5	-38833	4.53	13220	21876	12998	4000	8255
300.1	-38129	4.34	12717	20908	12240	3806	7499
262.4	-37426	4.14	12328	19946	11486	3628	6746
224.8	-36721	3.94	12012	18983	10737	3458	5999
187.8	-36024	3.75	11751	18027	9998	3295	5269
150.1	-35314	3.55	11527	17033	9239	3128	4525
112.7	-34600	3.35	11310	16007	8474	2959	3782
74.8	-33862	3.15	11089	14894	7667	2781	3022
37.4	-33118	2.95	10861	13683	6826	2586	2265
-0.0	-32349	2.74	10693	12296	5912	2376	1486
0.7	-32672	53.87	10760	12446	6078	2403	1509

Table 3: Experimental results for round hole specimen

Load	Gauge Number						
	6	7	8	9	10	11	12
kN	με	με	με	με	με	με	με
0.0	-159.6	252	591	-400	-451	-152	-137
37.5	469.8	626	964	197	104	417	390
75.1	1108.9	1015	1353	801	660	991	924
112.9	1760.8	1413	1744	1417	1233	1587	1481
150.0	2403.4	1814	2135	2026	1797	2176	2032
187.0	3063.6	2225	2530	2639	2360	2774	2594
224.8	3749.5	2637	2931	3282	2954	3402	3180
262.8	4477.9	3055	3329	3983	3586	4056	3795
299.9	5221.1	3460	3703	4801	4291	4735	4437
337.7	6011.9	3868	4046	6063	5254	5463	5140
374.9	7663.2	4248	4354	8675	6937	6339	5921
374.9	7733	4247	4352	8765	6981	6366	5934
375.0	7788.7	4246	4348	8834	7014	6389	5946
374.9	7833.8	4250	4349	8883	7038	6404	5952
375.0	7864.7	4248	4346	8923	7059	6419	5957
337.5	7200.2	3827	3931	8300	6476	5805	5377
300.1	6515.5	3406	3514	7647	5881	5185	4794
262.4	5835.1	2985	3097	7007	5295	4568	4213
224.8	5157	2565	2680	6364	4710	3957	3641
187.8	4494	2156	2273	5736	4138	3362	3084
150.1	3822	1745	1866	5096	3557	2756	2516
112.7	3152	1342	1467	4457	2980	2162	1958
74.8	2470	938	1065	3793	2387.	1560	1397
37.4	1799	554	681	3118	1785	966	846
-0.0	1110	176	30	2415	1168	376	298
0.7	1115	-100	-93	2590	1364	365	263

Table 4: Experimental results for round hole specimen

LOAD	Strip Gauge Element				
	s_1	s_2	s_3	s_4	s_5
kN	με	με	με	με	με
0.0	-27	-98	-191	-289	-363
37.5	-82	180	437	692	902
75.0	-138	459	1073	1684	2169
112.9	-198	737	1709	2689	3458
149.9	-258	1010	2341	3709	4749
187.0	-316	1283	2957	4709	5989
224.7	-413	1501	3495	5545	7090
262.8	-573	1626	3874	6116	8458
299.8	-826	1619	4079	6533	10132
337.7	-1205	1475	4155	6960	12157
374.9	-1884	906	3739	7003	15521
374.9	-1908	872	3700	6977	15626
374.9	-1928	844	3671	6952	15714
374.8	-1944	825	3652	6939	15780
375.0	-1958	807	3632	6931	15836
337.5	-1919	502	2965	5897	14519
300.0	-1864	217	2316	4881	13170
262.4	-1811	-63.	1682	3880	11838
224.8	-1749	-336	1053	2892	10506
187.7	-1685	-599	448	1939	9200
150.1	-1613	-853	-145	1004	7857
112.7	-1532	-1088	-703	114	6502
74.8	-1432	-1302	-1232	-733	5092
37.4	-1310	-1479	-1708	-1515	3657
-0.0	-1166	-1620	-2129	-2230	2180
0.7	-1110	-1524	-1987	-2045	2385

Table 5: Experimental results for round hole specimen

LOAD	Strip Gauge Element				
	s_6	s_7	s_8	s_9	s_10
kN	με	με	με	με	με
0.0	-414	-420	-353	-252	-138
37.5	1099	1199	1246	1207	1084
75.0	2614	2823	2862	2684	2321
112.9	4169	4484	4531	4198	3578
149.9	5729	6152	6206	5711	4831
187.0	7377	8204	8230	7292	6039
224.7	9601	11230	11163	9358	7056
262.8	12552	15367	15187	12049	8261
299.8	16279	20926	20442	15367	9659
337.7	21627	29241	28214	20069	11260
374.9	33594	36759	43158	29884	13661
374.9	33991	36941	42947	30063	13706
374.9	34308	37067	43004	30040	13755
374.8	34549	37065	42562	30103	13790
375.0	34745	37101	42230	30097	13819
337.5	33029	35808	40622	28292	12538
300.0	31304	34577	39389	26637	11243
262.4	29639	33374	38192	25084	9955
224.8	27983	32176	36985	23539	8680
187.7	26327	31005	35777	21994	7426
150.1	24563	29781	34482	20361	6155
112.7	22689	28453	33092	18653	4894
74.8	20611	26934	31509	16769	3608
37.4	18325	25222	29750	14744	2335
-0.0	15769	23368	27860	12505	1051
0.7	15987	23564	28037	12614	1096

The clip gauge gives the overall compliance of the test specimen as shown in Figure 9, and was required to ensure the specimen finite element model was calibrated for the analysis prior to attempting correlation with all the gauges. Note that the initial zero value of -30,481 με from Table 2 has been subtracted from the strains plotted in Figure 9.

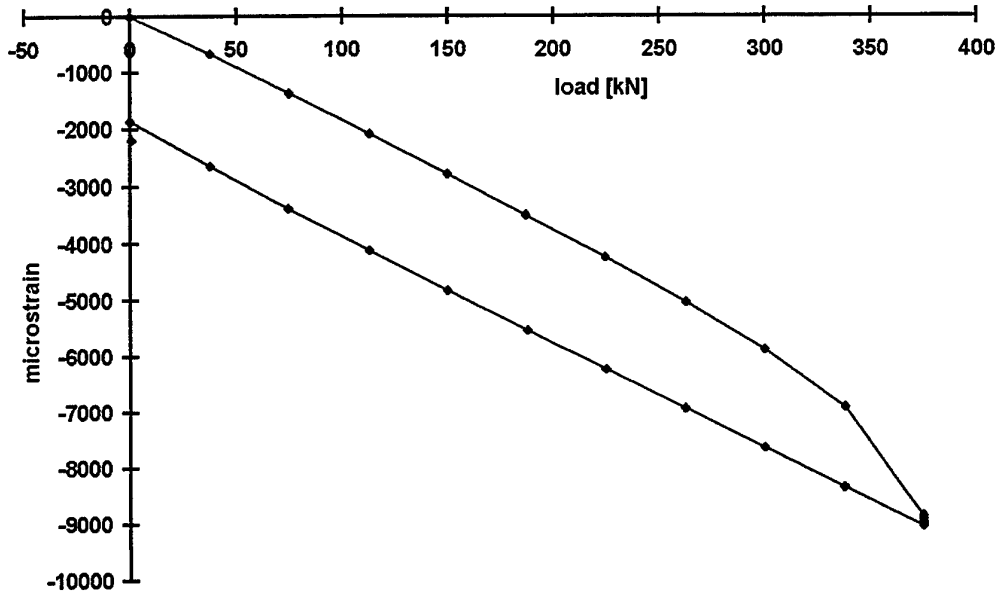

Figure 9: Clip gauge response

The strain versus load results for all strain gauges are plotted in Figures 10 to 16. Figures 10 & 12 show the gauge failure that occurred at 375 kN due to high strains, while Figures 15 & 16 show that higher strain levels could be sustained by the strip gauge without gauge failure.

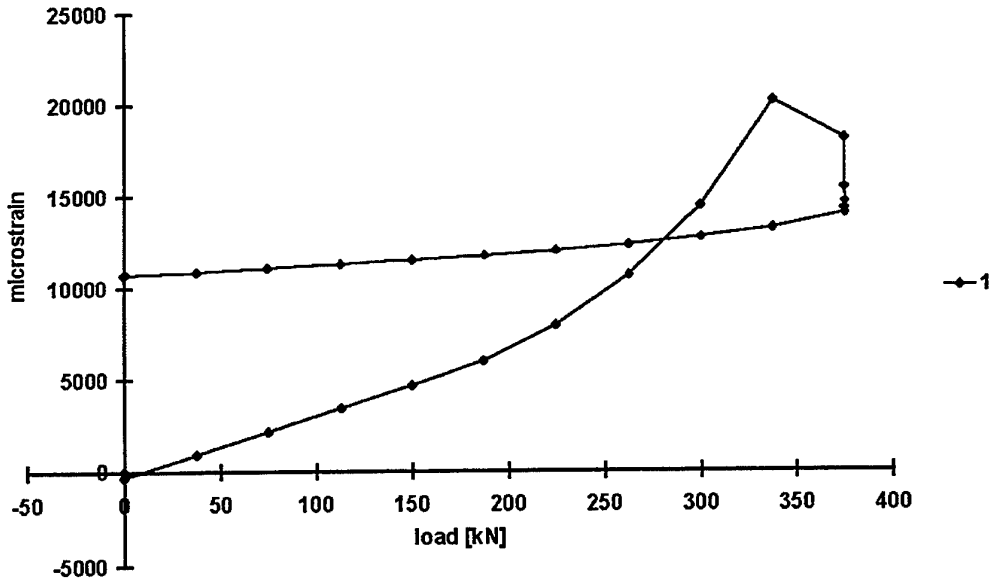

Figure 10: Response of gauge 1 on centre line

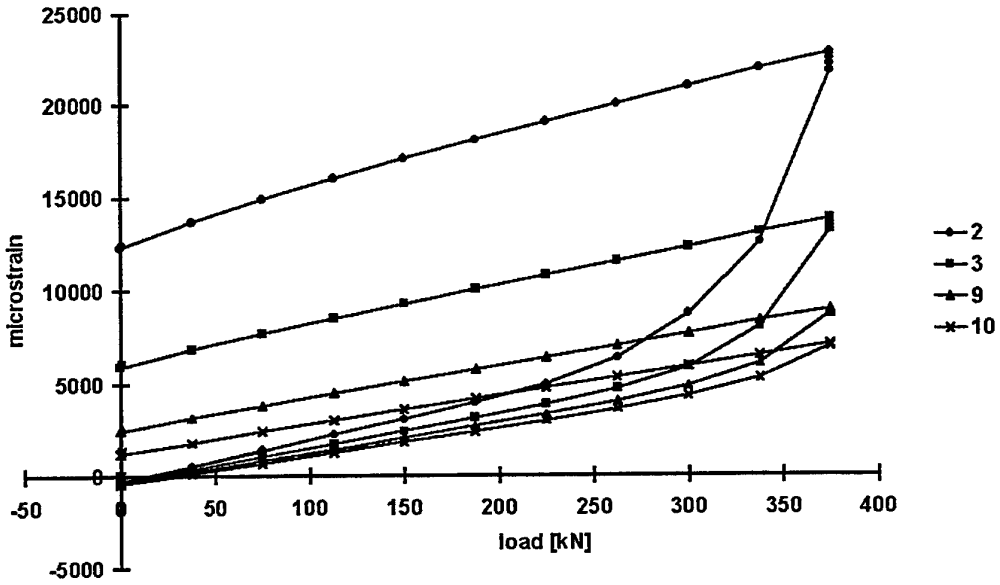

Figure 11: Response of gauges 2, 3, 9 & 10 on centre line

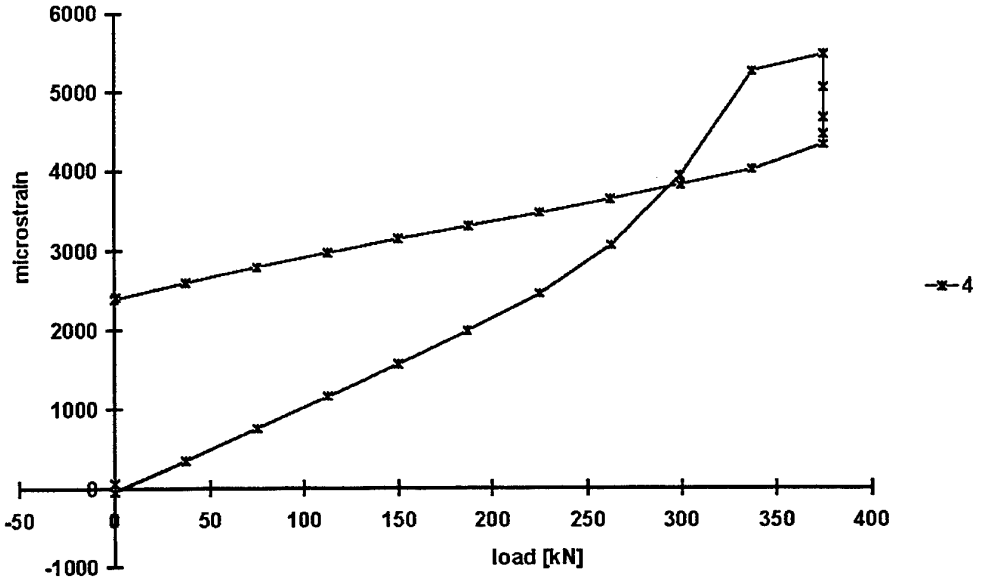

Figure 12: Response of gauge 4 on 63° line

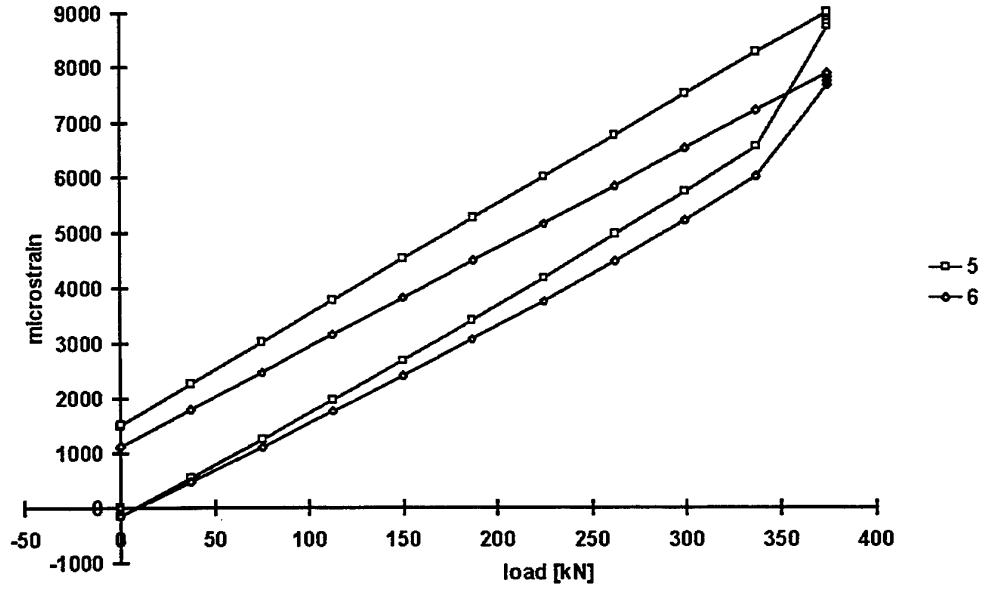

Figure 13: Response of gauges 5 and 6 on 63° line

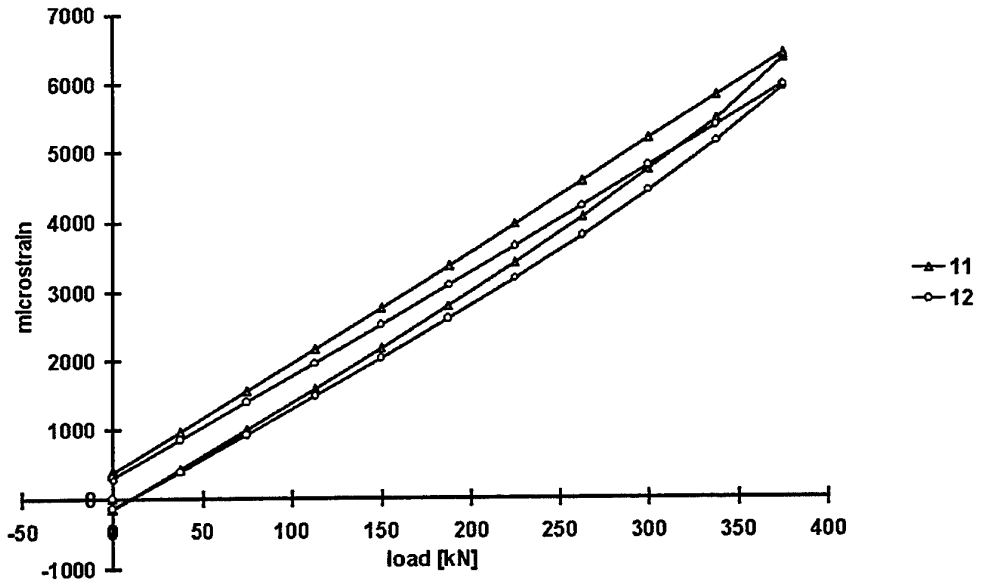

Figure 14: Response of gauges 11 & 12 on 63° line

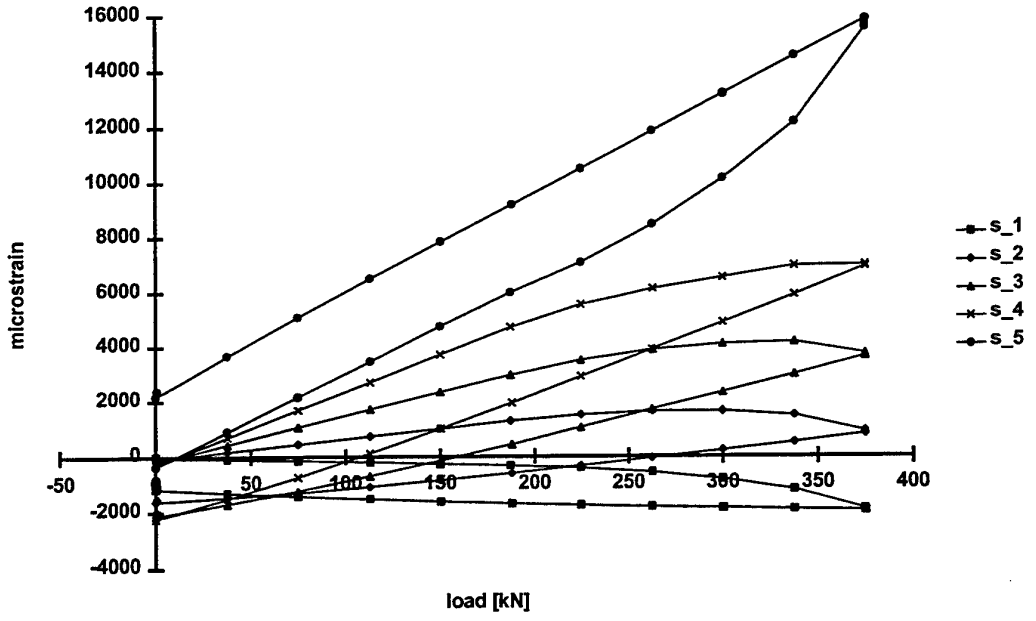

Figure 15: Response of strip gauge inside hole, gauge elements 1 to 5

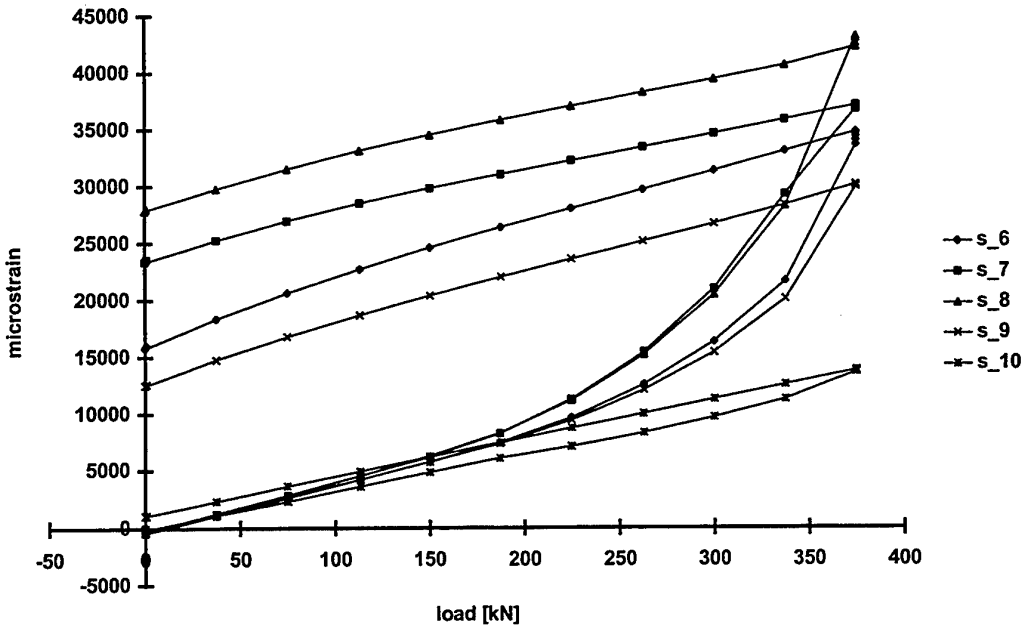

Figure 16: Response of strip gauge inside hole, gauge elements 6 to 10

7. Comparison of Test Results with Finite Element Method

The finite element model calibration was checked for the overall compliance of the specimen against the clip gauge results. The comparative results are plotted in Figures 17 and 18 for classical and unified plasticity models respectively. The two finite element strains shown in each figure represent the nominal strains between the inner and outer edges of the aluminium blocks. The clip gauge results cannot be considered definitive because of the averaging of strain across the attachment block. Despite this, good correlation between finite element analysis and experimental clip gauge data was achieved, and considered satisfactory.

The classical plasticity analysis indicated that the strain measured by the clip gauge was the average of the strains between the inner and outer edges of the blocks, while the unified constitutive analysis indicated it was closer to the inner edge strain.

Note: The finite element analysis result at 375kN is not reliable because of numerical errors encountered in this load step. Results are plotted for reference only.

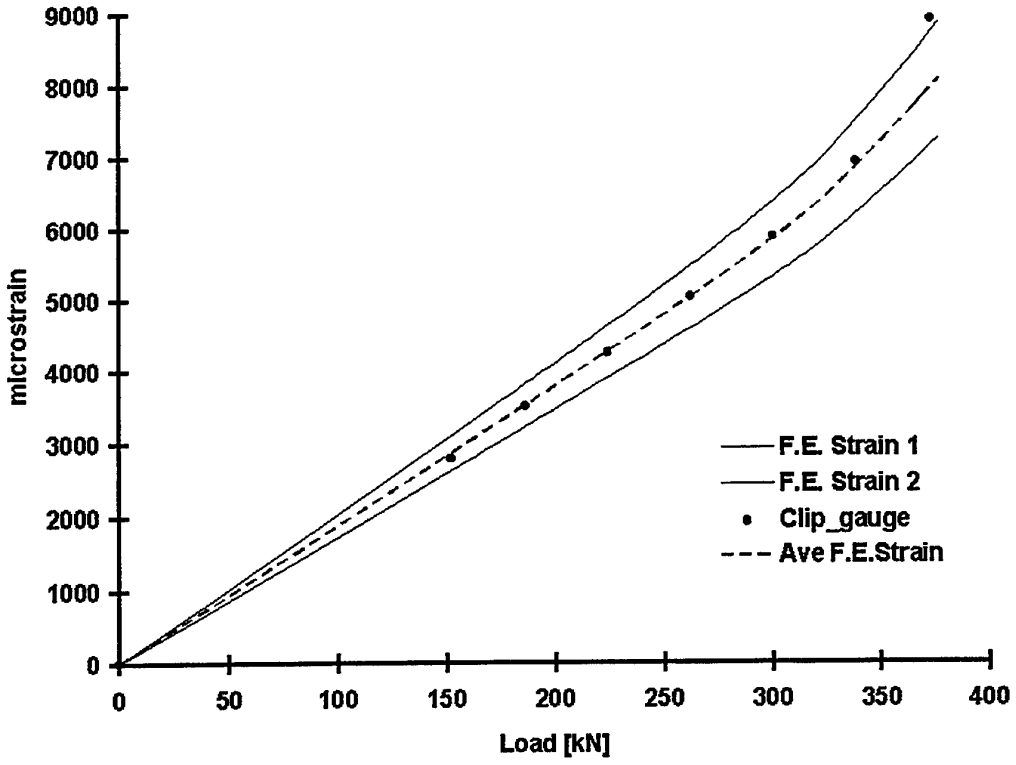

Figure 17: Comparison of clip gauge with classical plasticity finite element analysis

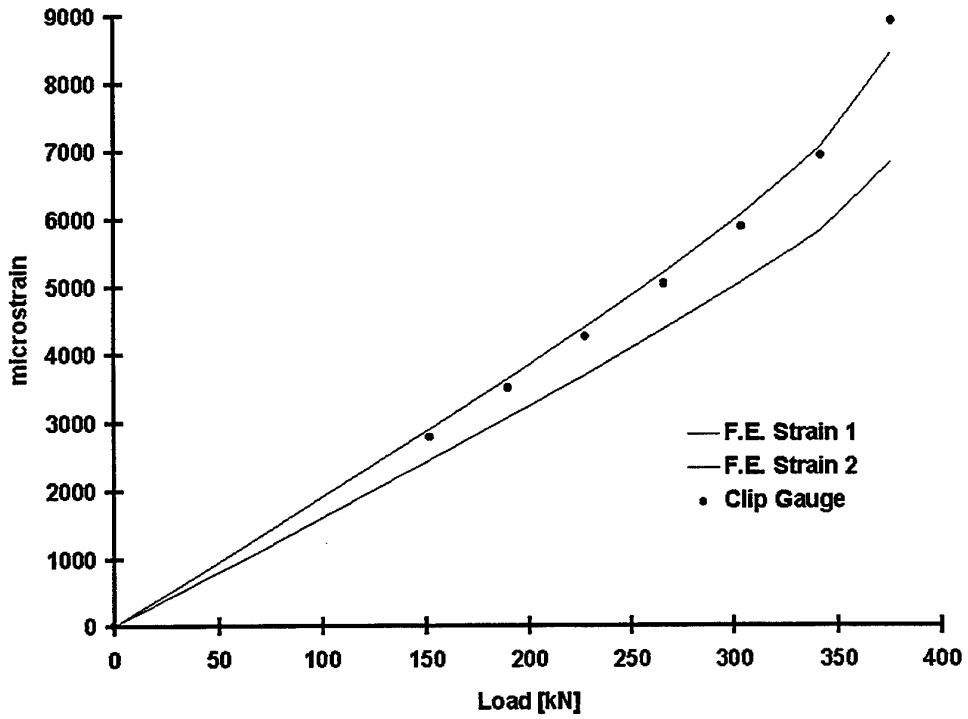

Figure 18: Comparison of clip gauge with constitutive plasticity finite element analysis

Strain gauge comparisons are presented here in two ways. Gauges on the horizontal centre-line are plotted for load steps as strain distributions and compared to both classical and unified constitutive finite element results (Figures 19, 20, 21 and 22). Gauges number 3 and 10 on the horizontal centre-line are also plotted as load versus strain and compared to similar finite element determined results (Figures 23 & 24). The strip gauge results from around the hole radius are plotted and compared to finite element results for one load step at 262 kN (Figure 25) - this was chosen as it is close to the maximum, just before the single gauges 4 and 1 failed.

The load versus strain responses of the other gauges were not plotted as they were not co-incident with nodes in the finite element mesh and correlation was difficult. Enough data were obtained without needing these gauges.

The strain distribution along the specimen centre-line, as shown in Figure 19 for a load of 156 kN, is essentially elastic. It can be seen that both finite element analyses over-predict the elastic strain. This may be due to the plain stress asumption used in the analyses. However, at the higher load levels of 262 kN and 342 kN shown in Figures 20 & 21, at which plasticity had developed at the edge of the hole, the agreement was better and the unified constitutive finite element analysis agreed very closely. Similar close agreement between unified constitutive finite element analysis and the

experimental strain data is shown in Figure 25 for the hoop strain distribution around the hole at 262 kN.

Figure 22 shows that the classical and unified constitutive finite element analyses significantly under-predicted the strain at very high load and associated high plasticity. In the case of the unified constitutive finite element analysis, the under-prediction may be due to the very high strains at the edge of the hole (43,000 με for gauge element S_8) being beyond the strain range for which the unified constitutive model parameters were derived [1]. The strain versus load responses for gauges 3 & 10 shown in Figures 23 & 24 respectively are also seen to be predicted better by the unified constitutive finite element analysis than the classical finite element analysis.

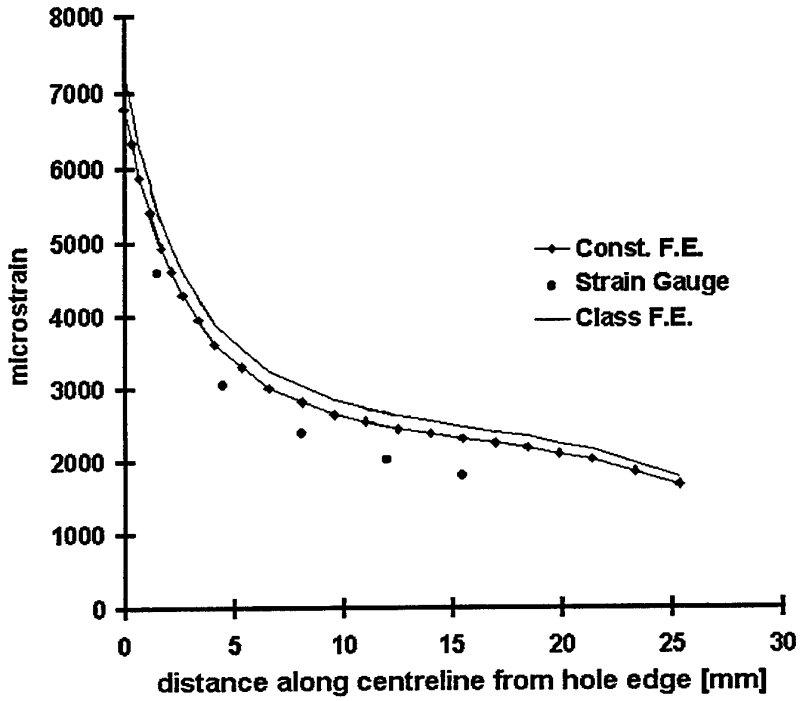

Figure 19: Experiment, constitutive plasticity F.E. and classical plasticity F.E. at 156kN

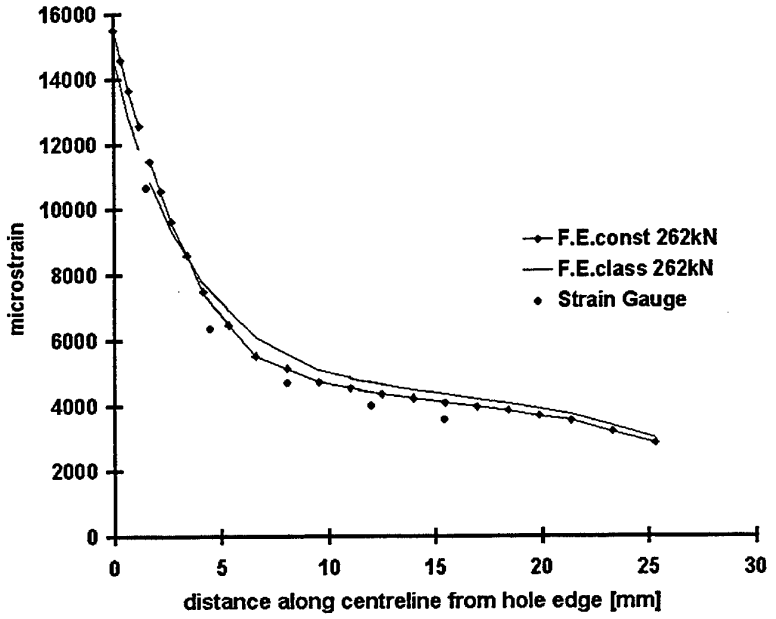

Figure 20: Experiment, constitutive plasticity F.E and classical plasticity F.E. at 262kN

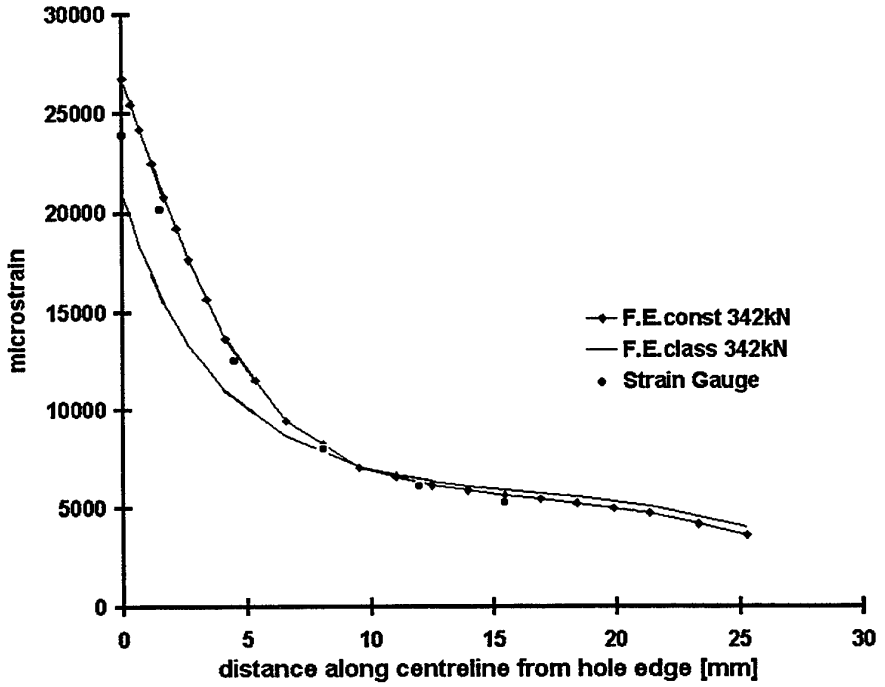

Figure 21: Experiment, constitutive plasticity F.E. and classical plasticity F.E. at 342kN

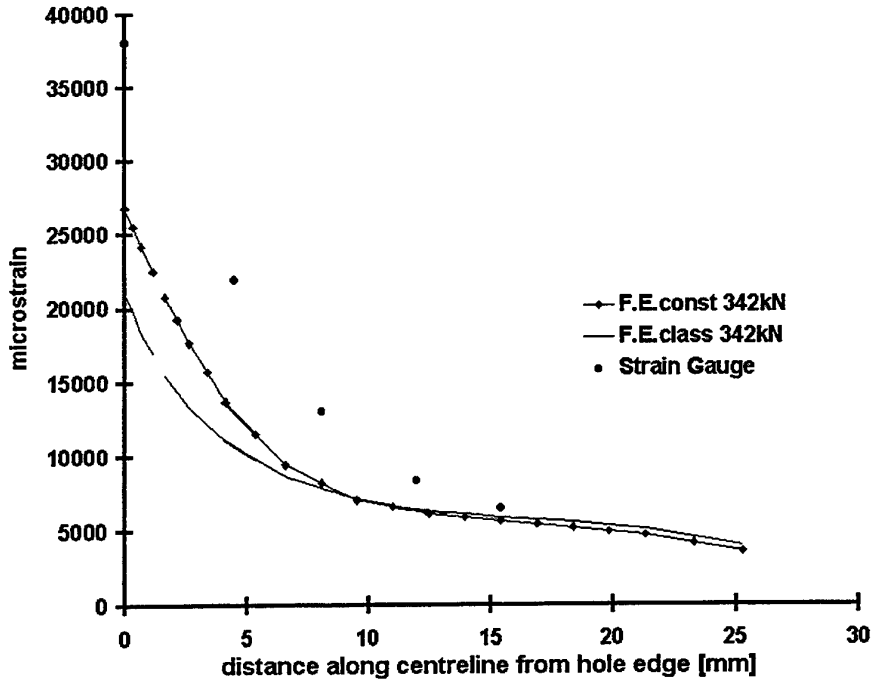

Figure 22: Experiment, constitutive plasticity F.E and classical plasticity F.E. at 376kN

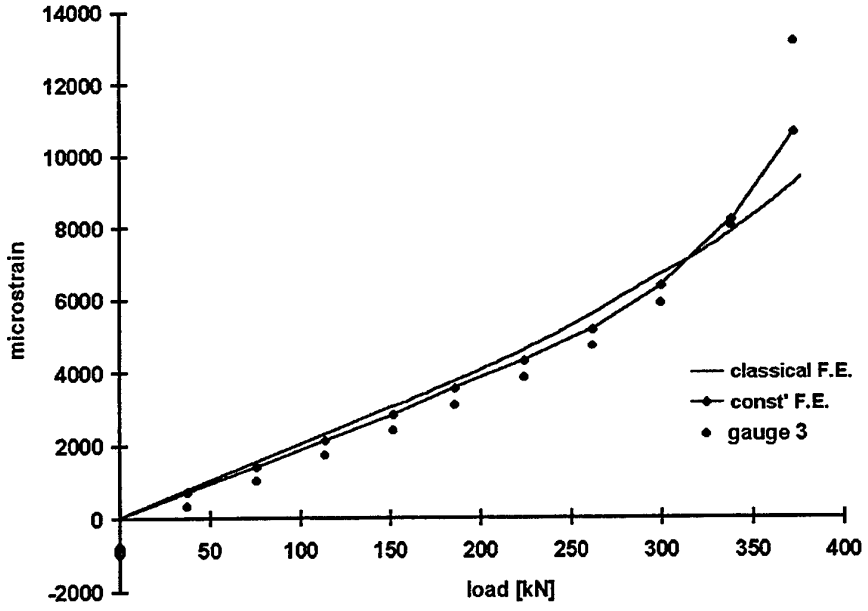

Figure 23: Comparison of strain gauge number 3 (8mm from hole edge) with constitutive plasticity F.E. and classical plasticity F.E.

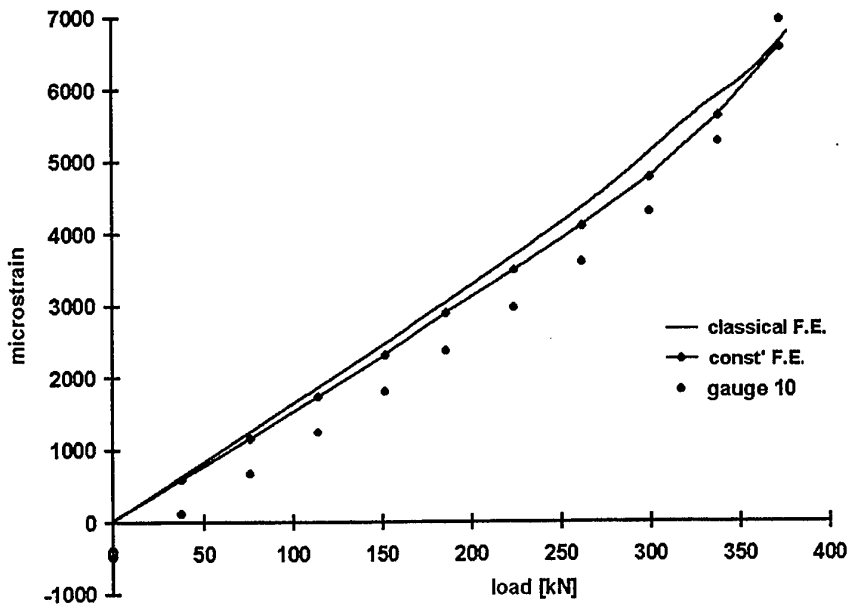

Figure 24: Comparison of strain gauge number 10 (15.5mm from hole edge) with constitutive plasticity F.E. and classical plasticity F.E.

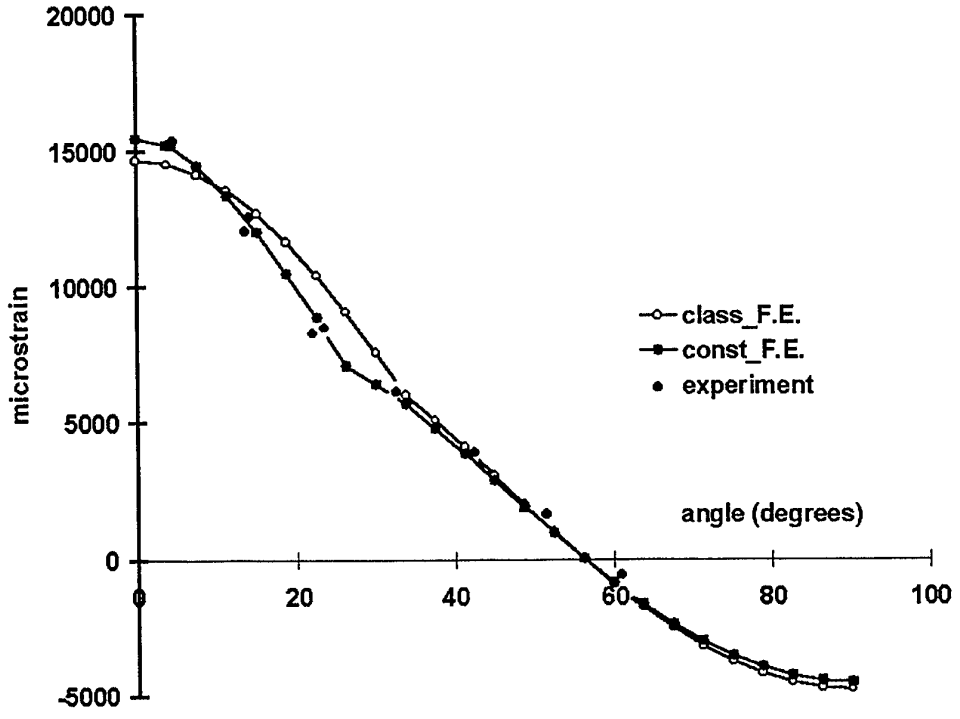

Figure 25: Comparison of strip strain gauge elements with constitutive plasticity F.E. and classical plasticity F.E at 262kN

8. Photoelastic Results

Photoelastic results were to be used as a back-up for strain gauge results. As the strain gauge results were considered to be good, no further work was done on post-processing the photoelastic results. Presented in this section are the fringe patterns for 75 kN, 150 kN, 337 kN and 375 kN.

These results show the plastic strains developing as expected.

Note: The 375 kN result shows the break down in the photoelastic coating adhesive layer at the higher strain levels.

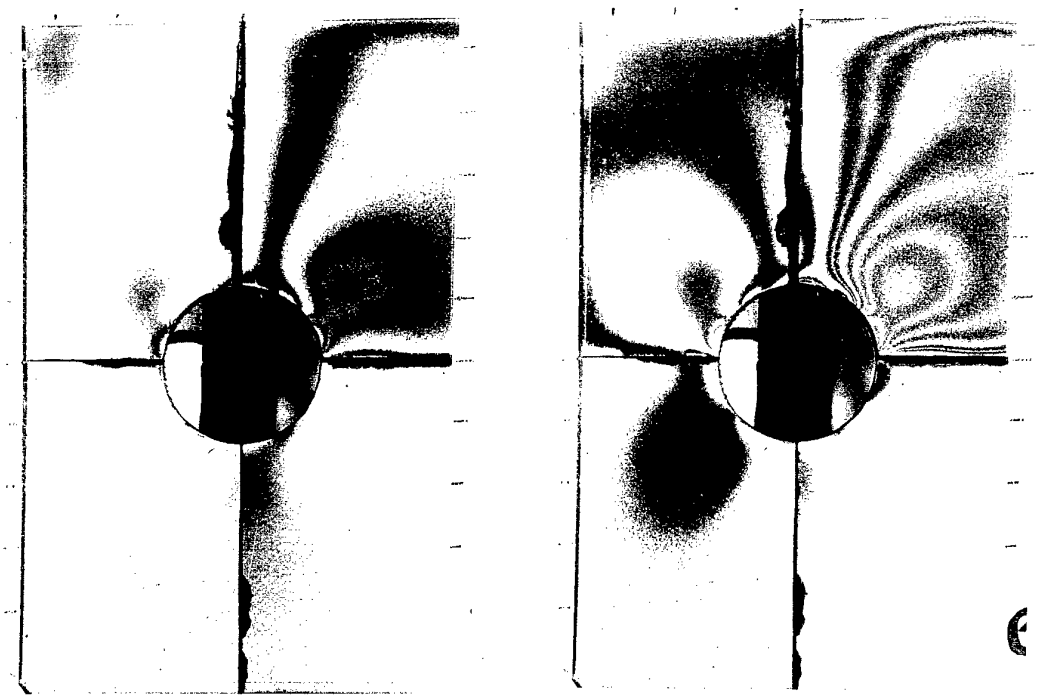

Figure 26: Photoelastic stress distribution at 75kN & 150kN.

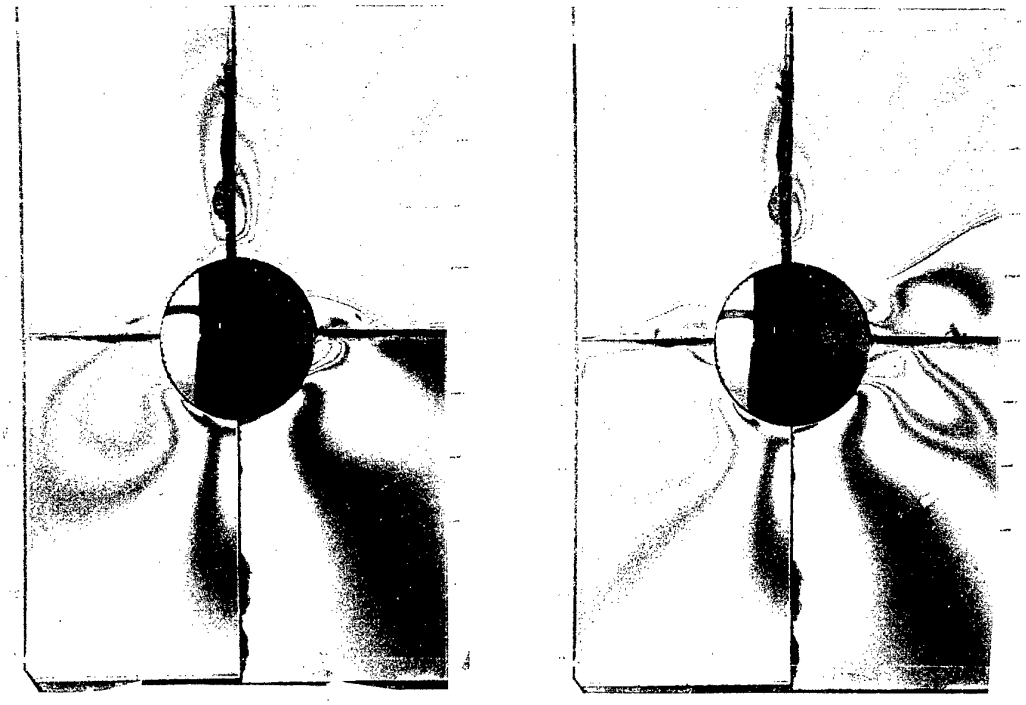

Figure 27: Photoelastic stress results at 337kN and 375kN.

9. Conclusion

This report has validated, for monotonic tensile loading, the unified constitutive material model for D6ac steel in PAFEC level 8.1. The validation was done on a two-dimensional specimen comprising a hole in a plate, and at strain rates close to those for which the material constitutive behaviour was characterised in essentially uniaxial stress fields.

An experimental stress analysis of a strain gauged flat plate specimen with a central circular hole was undertaken. The specimen was loaded monotonically in tension to 375 kN, then unloaded to zero load.

Comparisons of finite element and strain gauge results were done via load versus strain responses at specific gauge locations and via strain distributions around the hole at specific load levels. Excellent correlation was obtained between experimental strain gauge results and finite element results using the unified constitutive material model in PAFEC level 8.1.

Best results were obtained when the levels of plasticity were high, eg Figure 21 at 342 kN. But, at lower levels of plasticity and at full elasticity, correlation was still high

and the unified constitutive material model was consistently better than the classical plasticity model, eg. Figure 20 at 262 kN and Figure 19 at 156 kN. At very high levels of plasticity both finite element analyses significantly under-predicted the experimental strains (Figure 22) and it may be concluded that they become inaccurate beyond 25,000 με.

Classical plasticity material parameters used were from Reference 8 and were not checked. This report did not investigate the classical plasticity response of the plate specimen using plasticity material parameters derived from the data presented by Searl & Paul [1]. The lower correlation of the classical plasticity results with the experimental data could be due to less precise material data sourced from [8].

Validation of the elastic-plastic boundary was not attempted, but could be the subject of further work as it provides a full field experimental stress analysis tool that has wider uses, eg cold working, cold expansion, interference fitting, etc.

10. Acknowledgments

The author wishes to acknowledge the valued contributions from the following people: Kevin Watters for valuable additions to this report and along with Francis Rose for helpful discussions, Julian Paul for assistance in finite element modelling and Michael Ryan for conducting the tests.

11. References

[1] **SEARL, A. and PAUL J.,** *Characterisation of D6ac steel using a unified constitutive model,* AMRL Report to be published, file M1/8/982

[2] **PAUL, J.,** *Final report on the implementation of a unified constitutive model into the PAFEC finite element package,* by, AMRL, 1996.

[3] **PAUL, J., CHAPMAN, P. and SEARL, A.,** *Elastic/plastic finite element analysis of the F-111C fuel flow vent hole number 13,* DSTO-TR-0454, AMRL Report, November 1996.

[4] **COCHERHAM, G. and EATON, D.E.,** *An estimation of plastic zones in a plate with a central hole,* 'STRAIN', October 1976.

[5] **THEOCARIS P.S. and MARKETOS E.,** *Elastic-plastic analysis of perforated thin strips of a strain hardening material,* J.Mech.Phys.Solids, 1964, Vol 12 pp377 to 390.

[6] **LILLINGTON, K.** *F-111 wing variable sweep strain survey,* Structures Laboratory Report N0 8/95, 1995, AMRL.

[7] **ILETT, J.V.** *Strain gauge locations - F-111 wing pivot fitting,* Drawing No. SE5/52/14/RS100, Revision 3, AMRL.

[8] **MOLENT, L. and SWANTON, G.,** *F-111 fuel flow hole #13 strain surveys,* ARL Technical Note 33, 1993.

Appendix A:

PAFEC Data File - Classical Plasticity

```
C file PLATE01PL1.DAT
C ROUND HOLE
C Plasticity test run #1
C Loaded to 990MPa in steps of:
C
CONTROL
FULL.CONTROL
PHASE=1
PHASE=2
PHASE=4
PHASE=6
PHASE=7
PLASTICITY
PHASE=9
BASE=5550000
STOP
CONTROL.END
NODES
NODE.NUMBER        X              Y
    1              0              12.7
    2              4.86008        11.73327
    3              8.98026        8.98026
    4              11.73327       4.86008
    5              12.7           0
    6               38            0
    7              0              50
    8               38            50
    9              0              90
    10             38             90
C
PAFBLOCKS
TYPE=1
BLOCK.NUMBER  GROUP.NUMBER  N1  N2  ELEMENT.TYPE  PROPERTIES TOPOLOGY
  1        1        1  5  36210        11     1 3 7  8 2
  2        1        2  6  36210        11     3 5 8  6 4
  3        1        3  7  36210        11     7 8 9 10
C
MESH
REFERENCE SPACING.LIST
1       12
2       12
3       12
4       1
5       0.35 0.5 0.5 0.75 1.25 1.5 1.5 1.5 1.5 1.5 2
```

```
6       0.35 0.5 0.5 0.75 1.25 1.5 1.5 1.5 1.5 1.5 2
7       6
8       12
C
MATERIAL
MATERIAL.NUMBER   E       NU
11                205E3           0.3
C
RESTRAINTS
NODE.NUMBER  PLANE   DIRECTION
1                1               1
5                2               2
C
PLATES.AND.SHELLS
PLATE.NUMBER   MATERIAL.NUMBER    THICKNESS
11                      11                5.0
C
C
TOLERANCES
REFERENCE TOL5
1       5.0
C
STATE.DETERMINATION
ALGOR TOL  PATH
 1  1E-3  1
C
C
PLASTIC.MATERIAL
PLASTIC.MATERIAL YIELD.CRITERION UNIAXIAL.PROPS
   11                   1                11
C
C
C  DATA FOR TENSILE STRESS-STRAIN CURVE USED !!
UNIAXIAL.PROPS
UNIAXIAL  TYPE  PROPERTY
  11      1   1142.00, 89.00E3
            1197.00, 72.00E3
            1246.00, 23.00E3
            1269.00, 19.00E3
            1288.00, 16.00E3
            1320.00, 13.50E3
            1347.00, 11.00E3
            1369.00, 8.500E3
            1386.00, 7.500E3
            1401.00, 6.000E3
            1413.00, 4.500E3
            1431.00, 2.500E3
            1441.00, 1.900E3
            1460.00, 1.400E3
            1474.00, 1.100E3
            1485.00, 0.850E3
```

```
            1502.00, 0.750E3
            1517.00, 0.600E3
            1529.00, 0.500E3
            1539.00, 0.450E3
            1548.00, 0.450E3
            1557.00, 0.250E3
            1567.00, 0.200E3
            1575.00, 0.125E3
            1580.00, 0.070E3
            1587.00, 0.030E3
C
C
YIELDING.ELEMENTS
PLAS GROUP
 11             1
C
C
CONVERGENCE
LOAD MAX.ITER QUIT  TOLERANCE
1              30     1                1
C
SURFACE.FOR.PRESSURE
PRESSURE.VALUE    NODE   PLANE
-100                9     2
C
INCREMENTAL
LOAD  STEP
 1    400 10 10 10 10 10 10 10 10 10
*     10 10 10 10 10 10 10 10 10 10
*     10 10 10 10 10 10 10 10 10 10
*     10 10 10 10 10 10 10 10 10 10
*     10 10 10 10 10 10 10 10 10 10
*     10 10 10 10 10 10 10 10 10 10
C
END.OF.DATA
```

Appendix B:

PAFEC Data File - Constitutive Plasticity

```
C file PLA01CON1A.DAT
C ROUND HOLE
C Constitutive Plasticity test run #1
C Loaded to 990MPa
C With Reduced Integration
CONTROL
FULL.CONTROL
PLASTICITY
CONSTITUTIVE
RUN.OPTIMISE
VECTORSOL
PHASE=1
PHASE=2
PHASE=4
PHASE=6
USE.NL0007
PHASE=7
PHASE=9
BASE=5550000
STOP
CONTROL.END
NODES
NODE.NUMBER   X          Y
   1          0           12.7
   2          4.86008     11.73327
   3          8.98026     8.98026
   4          11.73327    4.86008
   5          12.7        0
   6          38           0
   7          0           50
   8          38           50
   9          0           90
   10          38         90
C
PAFBLOCKS
TYPE=1
BLOCK.NUMBER  GROUP.NUMBER  N1  N2  ELEMENT.TYPE  PROPERTIES TOPOLOGY
  1        1      1  5  36210       11     1 3 7  8 2
  2        1      2  6  36210       11     3 5 8  6 4
  3        1      3  7  36210       11     7 8 9 10
C
MESH
REFERENCE SPACING.LIST
1     12
```

```
2       12
3       12
4       1
5       0.35 0.5 0.5 0.75 1.25 1.5 1.5 1.5 1.5 1.5 2
6       0.35 0.5 0.5 0.75 1.25 1.5 1.5 1.5 1.5 1.5 2
7       6
8       12
C
MATERIAL
MATERIAL.NUMBER    E      NU
11          205.0E3    0.3
C
RESTRAINTS
NODE.NUMBER   PLANE    DIRECTION
1         1      1
5         2      2
C
PLATES.AND.SHELLS
PLATE.NUMBER    MATERIAL.NUMBER     THICKNESS
11              11          5.0
C
C
TOLERANCES
REFERENCE TOL5
1      .05
C
STATE.DETERMINATION
ALGOR TOL  PATH
 1  1E-3  1
C
C
PLASTIC.MATERIAL
PLASTIC.MATERIAL YIELD.CRITERION UNIAXIAL.PROPS
   11         1          11
C
C
C  DATA FOR TENSILE STRESS-STRAIN CURVE USED !!
UNIAXIAL.PROPS
UNIAXIAL   TYPE   PROPERTY
  11       1    5200.00, 40000.0
C
YIELDING.ELEMENTS
PLAS  GROUP
 11    1
AUTOMATIC.CONTROL
AUTO=1
TOTA=2000
OUTPUT=0
TABLE=1
NUMB=1
DELTA=3
```

```
INIT=100
ABORT=.75
RE.FACTOR=.8
EX.FACTOR=1.3
RE.ITERATION=4
EX.ITERATION=2
MAXIMUM.TIME.STEP=100
BLOC
25
C
C
CONSTANTS.NEW.FLOW.LAW
MATE TYPE TEMP E     NU D   N   Z0 Z1   M   F1 F2 OMMAX
C EXPERIMENTALLY EVALUATED CONSTANTS BY ASH
C MONOTONIC
 11   1   25. 205000. 0.32 10000. 3.  347.  347. 120.  30.0  0.8645 1510.
C
INCREMENTAL
LOAD  STEP
 1   990
C
TOTAL.TIME.VERSUS.FORCE.DATA
LOAD  LIST
 1   990
C
UNIFIED.CONTROL
JACOBIAN=2
METHOD=22
OOH.=.6
REEPSI REOMI REWRKI REQEPSI AEEPSI AEOMI AEWRKI AEQEPSI
5E-8  5E-8 5E-8  5E-8   1E-11 1E-6 1E-12 1E-11
C
C    5E-8  6 REEPSI - allowable relative error on EPSI  C
C    5E-8  6 REOMI  - allowable relative error on OMI   C
C    5E-8  6 REWRKI - allowable relative error on WRKI  C
C    5E-8  6 REQEPSI- allowable relative error on QEPSI C
C    1E-11 9 AEEPSI - allowable absolute error on EPSI  C
C    1E-6  4 AEOMI  - allowable absolute error on OMI   C
C    1E-12 10 AEWRKI - allowable absolute error on WRKI  C
C    1E-11 9 AEQEPSI- allowable absolute error on QEPSI C
C
CONVERGENCE
LOAD MAX.TER TOLER  C  FREQ   FIX.
 1  8            1   C  2    5.
C
C
CONVERGENCE
LOAD  MAX.ITER  QUIT   TOLERANCE
1               30      1                1
C
SURFACE.FOR.PRESSURE
```

```
PRESSURE.VALUE    NODE    PLANE
-100              9       2
C
C
END.OF.DATA
```

DISTRIBUTION LIST

Elastic-Plastic Analysis of a Plate of Strain Hardening Material with a Central Circular Hole - Comparison of Experiment with Finite Element Analysis Containing the Unified Constitutive Material Model

Robert B. Allan

DEFENCE ORGANISATION

Task Sponsor AIR OIC ASI-LSA

S&T Program

Chief Defence Scientist
FAS Science Policy
AS Science Corporate Management
} shared copy

Counsellor Defence Science, London (Doc Data Sheet)
Counsellor Defence Science, Washington (Doc Data Sheet)
Scientific Adviser to MRDC Thailand (Doc Data Sheet)
Director General Scientific Advisers and Trials/Scientific Adviser Policy and Command (shared copy)
Navy Scientific Adviser (3 copies Doc Data Sheet and 1 copy distribution list)
Scientific Adviser - Army (Doc Data Sheet and distribution list only)
Air Force Scientific Adviser
Director Trials

Aeronautical and Maritime Research Laboratory
Director

Electronics and Surveillance Research Laboratory
Director

Chief of Airframe and Engines Division
Research Leader Fracture Mechanics
Research Leader Structural Integrity
K. Watters
J. Paul
R.B. Allan (10 copies)

DSTO Library
Library Fishermens Bend
Library Maribyrnong
Library DSTOS (2 copies)
Australian Archives
Library, MOD, Pyrmont (Doc Data sheet only)

Forces Executive
Director General Force Development (Sea) (Doc Data Sheet only)
Director General Force Development (Land) (Doc Data Sheet only)

Army
ABCA Office, G-1-34, Russell Offices, Canberra (4 copies)

Air Force
CENG 501 WING, AMBERLY

S&I Program
Defence Intelligence Organisation
Library, Defence Signals Directorate (Doc Data Sheet only)

B&M Program (libraries)
OIC TRS, Defence Central Library
Officer in Charge, Document Exchange Centre (DEC), 1 copy
*US Defence Technical Information Center, 2 copies
*UK Defence Research Information Centre, 2 copies
*Canada Defence Scientific Information Service, 1 copy
*NZ Defence Information Centre, 1 copy
National Library of Australia, 1 copy

UNIVERSITIES AND COLLEGES

Australian Defence Force Academy
Library
Head of Aerospace and Mechanical Engineering
Deakin University, Serials Section (M list), Deakin University Library, Geelong, 3217
Senior Librarian, Hargrave Library, Monash University
Librarian, Flinders University

OTHER ORGANISATIONS

NASA (Canberra)
AGPS

OUTSIDE AUSTRALIA

ABSTRACTING AND INFORMATION ORGANISATIONS
INSPEC: Acquisitions Section Institution of Electrical Engineers
Library, Chemical Abstracts Reference Service
Engineering Societies Library, US
Materials Information, Cambridge Scientific Abstracts, US
Documents Librarian, The Center for Research Libraries, US

INFORMATION EXCHANGE AGREEMENT PARTNERS
Acquisitions Unit, Science Reference and Information Service, UK
Library - Exchange Desk, National Institute of Standards and Technology, US
National Aerospace Laboratory, Japan
National Aerospace Laboratory, Netherlands

SPARES (10 copies)

Total number of copies: 68

DEFENCE SCIENCE AND TECHNOLOGY ORGANISATION
DOCUMENT CONTROL DATA

1. PRIVACY MARKING/CAVEAT (OF DOCUMENT)

2. TITLE

Elastic-Plastic Analysis of a Plate of Strain Hardening Material with a Central Circular Hole - Comparison of Experiment with Finite Element Analysis Containing the Unified Constitutive Material Model

3. SECURITY CLASSIFICATION (FOR UNCLASSIFIED REPORTS THAT ARE LIMITED RELEASE USE (L) NEXT TO DOCUMENT CLASSIFICATION)

Document	(U)
Title	(U)
Abstract	(U)

4. AUTHOR(S)

Robert B. Allan

5. CORPORATE AUTHOR

Aeronautical and Maritime Research Laboratory
PO Box 4331
Melbourne Vic 3001

6a. DSTO NUMBER	6b. AR NUMBER	6c. TYPE OF REPORT	7. DOCUMENT DATE
DSTO-TR-0492	AR-010-134	Technical Report	February 1997

8. FILE NUMBER	9. TASK NUMBER	10. TASK SPONSOR	11. NO. OF PAGES	12. NO. OF REFERENCES
M1/9/165		AIR OIC ASI-LSA	36	8

13. DOWNGRADING/DELIMITING INSTRUCTIONS

None

14. RELEASE AUTHORITY

Chief, Airframes and Engines Division

15. SECONDARY RELEASE STATEMENT OF THIS DOCUMENT

Approved for public release

OVERSEAS ENQUIRIES OUTSIDE STATED LIMITATIONS SHOULD BE REFERRED THROUGH DOCUMENT EXCHANGE CENTRE, DIS NETWORK OFFICE, DEPT OF DEFENCE, CAMPBELL PARK OFFICES, CANBERRA ACT 2600

16. DELIBERATE ANNOUNCEMENT

No limitations

17. CASUAL ANNOUNCEMENT Yes

18. DEFTEST DESCRIPTORS

Elastoplasticity, finite element analysis, plates, holes (openings), strain gages, photoelasticity

19. ABSTRACT

This report presents an experimental validation of elastic-plastic finite element stress analysis, using a unified constitutive model to describe the plastic response. The validation was done by experimentally measuring the elastic-plastic strain distribution around a circular hole in a flat plate under tensile loading and comparing it with that produced by a finite element analysis of the specimen using the unified constitutive model. The validation involved strain measurements using both strain gauges and full-field photoelasticity. The unified constitutive model was found to provide a significant improvement over classical plasticity modelling for the case of monotonic loading. A similar validation for cyclic plasticity has not yet been undertaken.

DISCLAIMER NOTICE

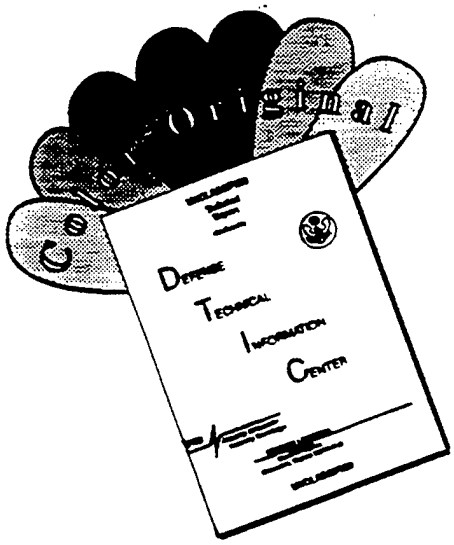

THIS DOCUMENT IS BEST QUALITY AVAILABLE. THE COPY FURNISHED TO DTIC CONTAINED A SIGNIFICANT NUMBER OF COLOR PAGES WHICH DO NOT REPRODUCE LEGIBLY ON BLACK AND WHITE MICROFICHE.